An Introduction to Time-Resolved Pump/Probe Spectroscopy

Article *in* Applied Spectroscopy · May 1985

DOI: 10.1366/0003702854248511

3 authors, including:

Fred Lytle
Indigo BioAutomation
135 PUBLICATIONS **2,904** CITATIONS

An Introduction to Time-Resolved Pump/Probe Spectroscopy

F. E. LYTLE,* R. M. PARRISH, and W. T. BARNES
Department of Chemistry, Purdue University, West Lafayette, Indiana 47907

The construction and operating principles of a two-color pump/probe spectrometer are described. This instrument is capable of obtaining ground-state absorption spectra, both singlet-singlet and triplet-triplet excited-state absorption spectra, photoproduct spectra, and stimulated fluorescence spectra. In addition, time-dependent measurements can be made with an impulse response of 250 ps and a free temporal range of 13 ns.

Index Headings: **Absorption spectroscopy; Fluorescence spectroscopy; Time-resolved spectroscopy; Lasers.**

INTRODUCTION

As the use of lasers in analytical fluorimetry increases, it has become apparent that methodological developments which emphasize specificity generally provide the most improved detection limits.[1-3] However, there are several classes of experiments where the signal is so drastically reduced in providing this selectivity that the sensitivity becomes marginal. With high directional resolution, the solid angle of the detection system intercepts only a very small fraction of the fluorescence emitted into 4π steradians. With high spectral resolution, the bandpass of the monochromator allows only a small fraction of emission wavelengths to reach the detector. And in an analogous manner, high temporal resolution reduces the fraction of the total decay contributing to the signal. In all three of these cases the problem is caused by the fact that fluorescence originates as a random process where the specific direction, wavelength, and time of creation that characterize any emitted photon are completely statistical. Thus, in analogy to common considerations in laboratory measurements, the computation of observational probabilities must include a specified uncertainty. That is, the intensity of a fluorescence signal must depend upon the value of the parameters $d\Omega$, $d\lambda$, and dt for the corresponding angular, spectral, and temporal uncertainties. The decrease in sensitivity with increased resolution is easily understood, since making one or more of these parameters equal to zero would result in complete loss of the signal.

In contrast to this situation, an absorption spectrum is a second-order stimulated process. The spectrum is not a probability distribution. As the slit is narrowed on an absorption spectrophotometer, the molar absorptivity asymptotically approaches a fixed, wavelength-dependent value. Likewise, a stimulated emission spectrum is not a probability distribution and would behave in a manner identical to absorption, except that the interacting beam of light is amplified instead of attenuated. In both of these processes the properties of directionality, bandwidth, and temporal uncertainty are carried by the source and not the absorbing molecule. Using lasers to determine stimulated spectra should allow the best possible combination of $d\Omega$, $d\lambda$, and dt, since many such sources have diffraction-limited divergence in addition to Heisenberg-limited pulse widths.

In order to record stimulated spectra, one usually employs a pump/probe experiment. With such an approach one beam of photons, the pump, is used to redistribute molecular energy via absorption from the ground state into either another real state or a virtual level (e.g., for Raman spectra). A second beam of photons, the probe, is then used to interrogate the gain or loss imposed by this optically prepared sample. Both processes can easily be made to obey Beer's law. Although pump/probe instruments have been built utilizing cw lasers,[4] the desire for time resolution dictates some form of pulsed laser. Low repetition rate devices were first used in such experiments,[5] but poor pulse-to-pulse reproducibility and complicated electronics are distinct disadvantages of this approach. Ease of signal processing favors high repetition rate variants such as continuously mode-locked lasers.[6-8]

The area of continuously operating, pulsed pump/probe experiments has been adequately covered in two comprehensive reviews.[9,10] An examination of the literature cited in these articles suggests that one major distinction among the instruments is the number of independently tunable colors used to obtain the data. Most single-wavelength studies are dynamical in nature, while the utilization of two different wavelengths for pumping and probing are desirable for obtaining easily interpretable spectra. Again, an examination of the literature indicates that the majority of instruments having dual mode-locked lasers is still being used in some dynamical sense, where picosecond to femtosecond pulses are used to time-resolve various spectra. It should be noted, however, that several studies use the short duration pulses simply to enhance the cross-section of a nonlinear process.[11,12]

The particular instrument described in this paper utilizes a mode-locked argon-ion laser exciting a synchronously pumped cw dye laser. The fixed 514.5 nm output of the argon-ion laser is used to both drive the dye laser and pump the sample. The wavelength tunable output of the dye laser is then used to obtain probe spectra. This configuration has not been popular in dynamical studies because the time response is limited by the 250 ps width of the pump pulse. In addition, the configuration would not be suitable for nonlinear processes because of the poor temporal overlap of the pump and probe pulses. However, the design is simple as far as the genre is concerned and provides both real-state spectra and time resolution of sufficient quality to be useful in many areas of applied spectroscopy.

Received 29 August 1984.
* Author to whom correspondence should be sent.

0003-7028/85/3903-0444$2.00/0

The example chemical systems are comprised of organic molecules in fluid solution. As such, none of the measurements are intrinsically limited by high spatial, spectral, or temporal resolution. However, they represent previously studied systems that can be kept under control well enough to demonstrate the principles involved in obtaining the various types of stimulated spectra. Example fluorimetric experiments where pump/probe spectroscopy should excel would be those involving gas combustion studies, line narrowing techniques, and samples in highly quenching environments.

EXPERIMENTAL

Chemicals. All chemicals used for the studies reported here were obtained from Eastman Chemicals, and used without further purification. The solvent was absolute ethanol obtained from U.S. Industrial Chemicals.

Instrumentation. The instrument block diagram is shown in Fig. 1. The mode-locked argon-ion laser was a Coherent Radiation CR-8 fitted with Harris Corp. acousto-optics. Operating at 514.5 nm, this source provided a 77-MHz train of 250 ps pulses with an average power of 750 mW. A halfwave plate, PR_1, and a polarization based beamsplitter cube, BS_1, combined effectively to form a continuously variable power divider. The horizontal component passed through a long path delay before being modulated by a Coherent Associates Model 317 electro-optical modulator (EOM) operating at 10 kHz. The long path minimized the degradation of mode-locking due to reflective feedback.[13] This portion of the argon-ion laser beam constituted the pump. The vertical polarization component was used to synchronously pump a Coherent Model 490 dye laser whose end mirror was resituated an appropriate length down the optical table. The ~20-ps-wide pulsed output of the mode-locked dye laser served as the probe. Two dyes, rhodamine 6G and sodium fluorescein, provided a tuning range from 530 nm to 645 nm.

Phase adjustment between the two 77-MHz pulse trains was obtained by means of a variable-length, four-pass delay line. This optical component was constructed from three 1″ corner-cube prisms mounted on a 41″ stepping-motor-driven Velmex Unislide and one corner cube mounted on the bench. The probe beam was then sent through a broadband polarization rotator, PR_2, and collinearly combined with the modulated pump beam via a dichroic beamsplitter, BS_2.

Both the pump and the probe beams were brought to a focus at the center of the sample cell and then transferred to the monochromator, MONO, by means of an achromatic lens, L_1. The sample was contained in a 1-cm-path-length spinning Raman cell. The 3000-rpm cell rotation rate performs two functions. It reduces the ac thermal lens contribution to the signal and it permits the observation of long-lived species by sweeping out the observation volume about every 13 μs. The purpose of the 0.25 meter monochromator was to block the pump beam and allow only the probe radiation to reach the detector. The detector, PD, was an EG&G Model SHS-100 photodiode. The output from the photodiode was fed to a Princeton Applied Research Model 128 lock-in amplifier, LIA, referenced to the modulation waveform.

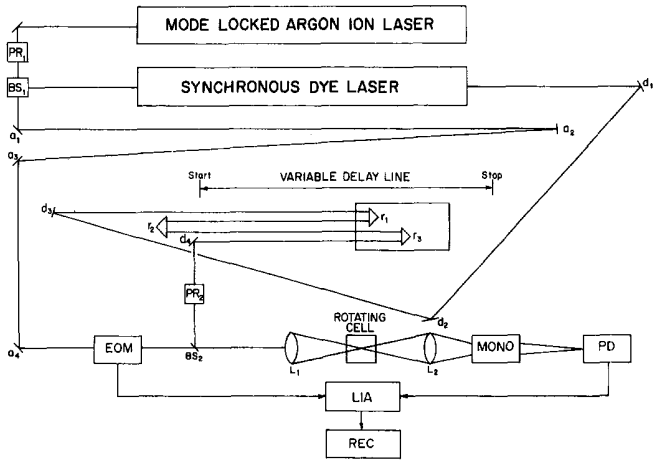

FIG. 1. Block diagram of the pump/probe instrument. a_1–a_4 are highly reflecting dielectric mirrors coated for the blue-green spectral region. d_1–d_4 are highly reflective dielectric mirrors coated for the orange-red spectral region. r_1–r_3 are uncoated quartz retro-reflecting prisms. The remaining components and the peculiar optical arrangement are described in the text.

Hard copy was obtained from a strip chart recorder, REC.

Data Treatment. To obtain a spectrum, we first set the delay line to the phase lag of interest and adjusted the dye laser wavelength by observing a diffuse reflection with a Bausch and Lomb spectroscope. At each wavelength, we observed the signal from the LIA output for 10–100 s to obtain some degree of signal averaging. To correct this raw data for probe power, we inserted a beamsplitter just prior to the photodiode, and a fraction of the beam was monitored by a Laser Precision Corp. Model RD3440 radiometer. Finally, the spectral response of the photodiode was measured and a table of correction factors was used to compensate for the effect of this component.

To obtain a decay, we first set the wavelength to the value of interest, and the length of the delay line was adjusted in a staircase fashion from one extreme to the other. Again, the LIA output was averaged for each step in the delay. To correct for the delay-dependent probe focal size in the sample cell, we first measured the signal for 3,3′-diethyloxadicarbocyanine iodide, DODCI. This compound has a signal strength which should be independent of the relative phase of the pump and probe beams. In practice, the signal for this compound decreases about 40% when going from a minimum to a maximum delay. Correction factors computed to force a flat DODCI response were subsequently used to convert raw decay data into the expected exponential functionality.

RESULTS AND DISCUSSION

Operating Principles. The concept behind the pump/probe experiment is very simple. Photons from the pump pulse are absorbed by the sample, causing a redistribution of the energy-state populations. At some arbitrary time with respect to pumping, a probe pulse irradiates this newly created population distribution. The measurement of interest is the difference in probe transmis-

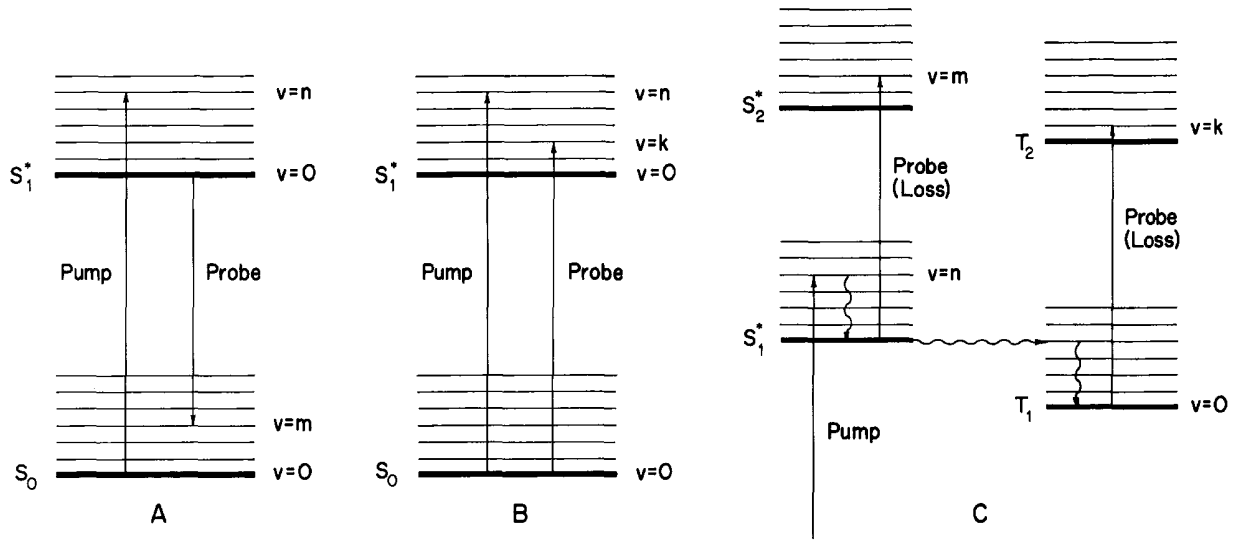

FIG. 2. Molecular vibronic state diagrams: A, probe energy corresponding to a fluorescence wavelength; B, probe energy corresponding to an absorption wavelength; C, probe energy corresponding to excited-state absorption wavelengths. The V labeling refers to hypothetical vibrational quantum numbers.

sion before and after pumping. This difference as a function of probe wavelength yields information about transition probabilities among various energy levels, and as a function of temporal pulse separation yields excited-state kinetic information.

To develop a quantitative feel for the operation of the instrument, consider first the probe interaction with the sample. Beer's law can be written in an exponential form as

$$I/I_0 = \exp[-2.3\epsilon b(C_1 - C_2)] \quad (1)$$

where C_1 is the concentration of the beginning energy level and C_2 is the terminating energy level for a transition having a molar absorptivity of ϵ. The parameter b is the effective sample path length. In the absence of rotational diffusion effects (achieved by the adjustment of the relative polarization of the two beams to the magic angle, 54.7°) and for a low value of absorbance, Eq. 1 can be rewritten in a loss form ($I < I_0$)

$$(1 - T) \simeq 2.3\epsilon b(C_1 - C_2) \quad (2)$$

or in a gain form ($I > I_0$) as

$$(T - 1) \simeq 2.3\epsilon b(C_2 - C_1). \quad (3)$$

As stated earlier, the primary function of the pump is to induce a change in the values C_1 and C_2. Thus, the measured probe interaction can be considered a variant of Eq. 3 having two parts,

$$(T - 1)_{\text{measured}} = (T - 1)_{\text{on}} - (T - 1)_{\text{off}} \quad (4)$$

where on and off denote the pump-on and pump-off portion of the chopping cycle.

Quantitative work is hampered in the present version of the instrument configuration by the utilization of only the lock-in output (ΔI, not $T - 1$) and by the employment of a single focusing lens instead of a collimating pair. The first change produces an output dependent on the probe power, while the second produces a pump photon flux density which varies across the length of the cell. These two complications make it difficult to directly measure absorptivities or concentrations. Nonetheless, straight line calibration curves can be constructed with a lower limit of detection near 5×10^{-7} M for the compounds utilized in this study. It should be noted that pump/probe experiments are ultimately source-shot-noise limited. This would predict a lower limit of detection at $(T - 1)_{\text{measured}} \sim 10^{-9}$ for the current instrument.

Ground-State/Excited-State Transitions. In a two-state emission experiment, the pump pulse is absorbed by the sample and promotes an $S_0(v = 0) \rightarrow S_1^*(v = n)$ transition (see Fig. 2A). If the probe pulse irradiates the sample within the excited volume created by the pump and corresponds to an emission wavelength of the sample, a fraction of the excited molecules will undergo $S_0(v = m) \leftarrow S_1^*(v = 0)$ stimulated fluorescence. The induced transitions add radiation coherently to the probe beam. Thus, as shown in Fig. 3B, the detector will record a modulation in phase with the pump. The depth of modulation will be proportional to the excited-state concentration, and by convention, the signal is taken to be positive. Thus, a relationship can be established between the probe amplification, emission-molar absorptivity, ϵ_e, and the energy level concentrations,

$$(T - 1)\alpha\epsilon_e[C_1^0(\text{on}) - C_0^m(\text{on})] - \epsilon_e[C_1^0(\text{off}) - C_0^m(\text{off})] \quad (5)$$

where the C_1^0(on, off) are the concentrations of the $v = 0$ vibronic level of the excited state during the pump-on and pump-off cycles, and the C_0^m (on, off) are the concentrations of the $v = m$ vibronic level of the ground state. For the situation where it can be assumed that the thermal population of $S_0(v = m)$ is negligible compared to $S_1(v = 0)$, Eq. 5 reduces to

$$(T - 1)\alpha\epsilon_e C_1^0(\text{on}) \quad (6)$$

since C_1^0(off) equals zero.

In a two-state absorption experiment, the probe wavelength corresponds to a $S_0(v = 0) \rightarrow S_1^*(v = k)$ transition

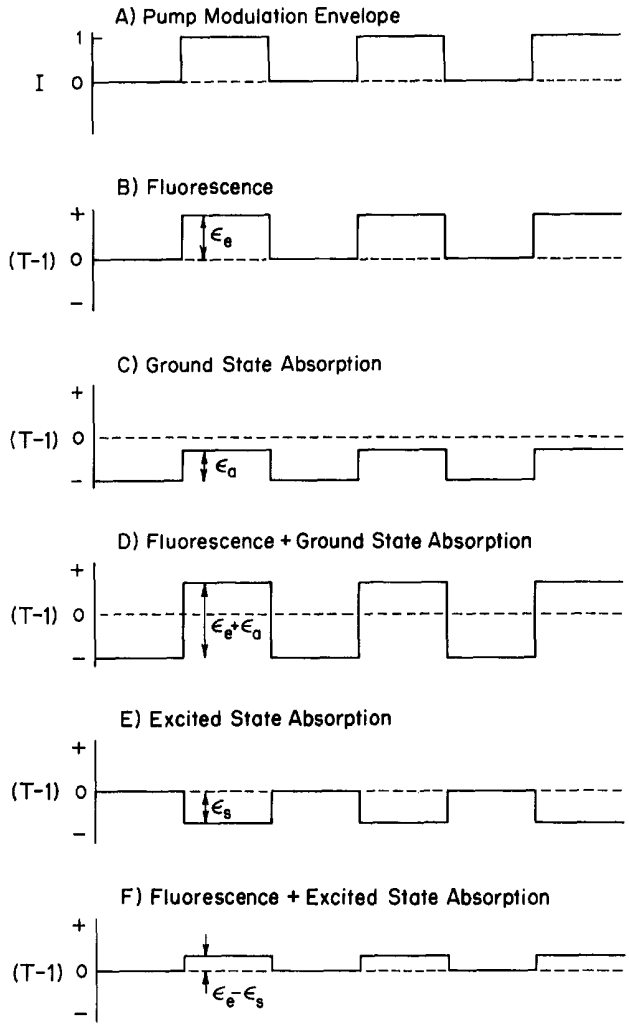

FIG. 3. Modulation envelopes for the pump (A) and probe (B–F) beams. Due to the operation of the lock-in amplifier, the induced probe modulation is taken to be positive when in phase with the reference (pump), and negative when 180° out of phase. Note that the envelope phase relationships have nothing to do with the pulse train phase relationships.

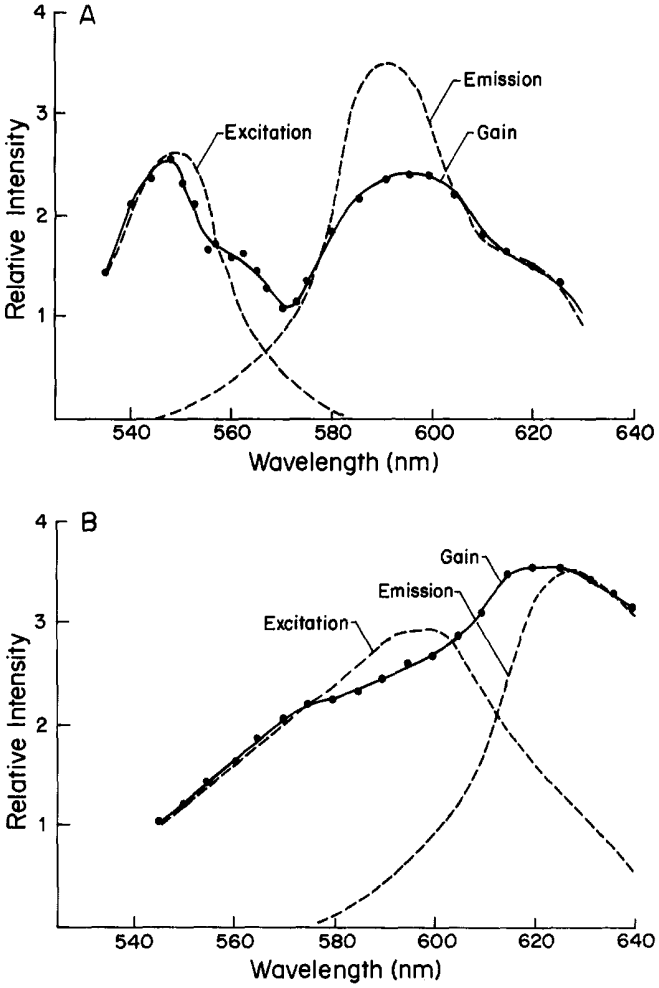

FIG. 4. Comparison of pump/probe gain spectra and spontaneous fluorescence excitation and emission spectra: A, acridine red; B, cresyl violet.

(see Fig. 2B). With the pump on, the ground-state population is depleted and the probe experiences a reduced absorption. Thus, as shown in Fig. 3C, the detector will again record a modulation in phase with the pump. The relationship between the probe amplification, absorption molar absorptivity, ϵ_a, and energy level concentrations can be written as

$$(T - 1)\alpha\epsilon_a[C_1^k(\text{on}) - C_0^0(\text{on})] - \epsilon_a[C_1^k(\text{off}) - C_0^0(\text{off})] \quad (7)$$

where the C_1^k(on, off) are the concentrations of the $v = k$ vibronic level of the excited state, and the C_0^0(on, off) are the concentrations of the $v = 0$ vibronic level of the ground state. For the situation where it can be assumed that the thermal population of $S_1(v = k)$ is negligible compared to $S_0(v = 0)$, Eq. 7 reduces to the following form:

$$(T - 1)\alpha\epsilon_a C_0^0(\text{off}) - \epsilon_a[C_0^0(\text{on})]. \quad (8)$$

This expression can be rewritten in terms of the excited-state concentration as

$$(T - 1)\alpha\epsilon_a C_0^0(\text{off}) - \epsilon_a[C_0^0(\text{off}) - C_1^0(\text{on})] \quad (9)$$

or simplified as

$$(T - 1)\alpha\epsilon_a C_1^0(\text{on}). \quad (10)$$

The result is a decrease in probe attenuation. That is, an apparent amplification which is instrumentally indistinguishable from a real amplification.

Because of thermal energy distributions in both the ground and excited states, and because of small Stokes' shifts in the 0-0 transition energies, it is possible to have finite values for both ϵ_e and ϵ_a at the same probe wavelength. For these cases the net amplification is proportional to

$$\epsilon_g C_1^0(\text{on}) = (\epsilon_e + \epsilon_a)C_1^0(\text{on}). \quad (11)$$

This is shown in Fig. 3D. However, the assumption that C_0^m and C_1^k are negligible can be incorrect. Thus, computing the expected magnitude of the signal in the wavelength region where absorption and fluorescence overlap could be difficult.

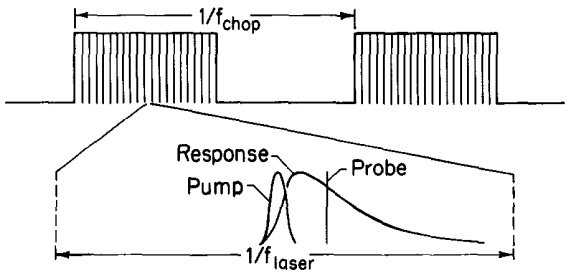

FIG. 5. Expansion of the time domain to show the pulsed nature of the experiment. The train of pump pulses is chopped at a frequency of f_{chop}, while the probe beam enters the sample with no modulation. The timing between the pump and probe beams is varied by means of the optical delay line. The free temporal range of the instrument, $1/f_{laser}$, is determined by the mode-locking frequency. The response is due to the concentration of excited states and not spontaneous fluorescence.

Pump/probe spectra having primarily gain transitions are worth examining. Figure 4A shows the pump/probe results for acridine red, along with normal excitation and emission data. As predicted, the measurement is approximately as sensitive to the absorption process as to stimulated emission. This conclusion is easily formulated since the gain peak at 547 nm is the result of ground-state absorption and is very close in intensity to the peak between 590 nm and 610 nm resulting from

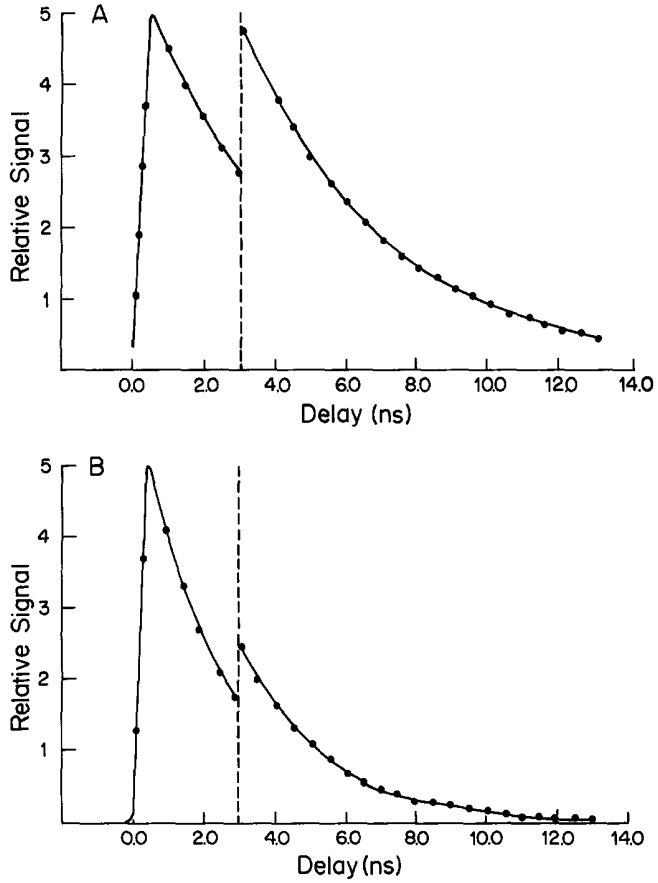

FIG. 6. Excited-singlet-state decays measured as the depth of induced probe modulation vs. the delay between the two beams: A, acridine red; B, cresyl violet.

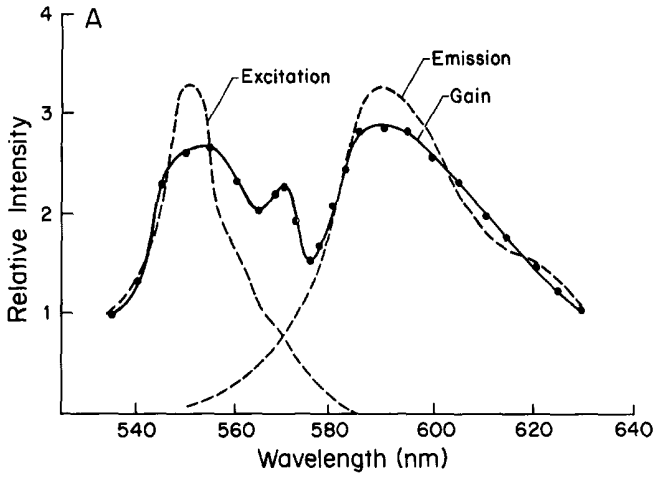

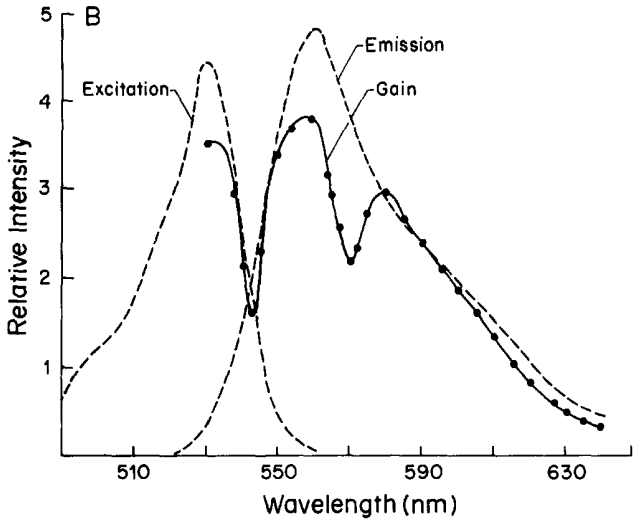

FIG. 7. Appearance of singlet-singlet absorption losses in a pump/probe gain spectrum: A, rhodamine B; B, rhodamine 6G.

stimulated emission. In addition, there exists a reasonable degree of correlation between the two sets of data. The only feature of the spectrum that appears noncharacteristic of the fluorescence curves is the shoulder at 560 nm. Figure 4B shows the same type of results for cresyl violet. Here the absorption peak isn't as clearly defined as that for acridine red. Additionally, the lack of any minimum near the 0-0 band is presumed to be due to the severe overlap of the normal excitation and emission spectra. It has been found empirically that low overlap of the normal spectra yields a deep minimum in the pump/probe curve.

Excited-State Decays. Because of the simple relationship between measured gain and S_1^0(on), excited-singlet-state decays can be monitored by varying the relative phase (delay time) between the pumping and probing pulse trains. The probe wavelength can be set to monitor excited-state decay or ground-state recovery. The temporal relationship between the 250-ps argon-ion pump pulse, the 20-ps dye pulse and the decay of the excited-state concentration is shown in Fig. 5. Due to the 10-kHz chopping rate, this process is repeated ~4000 times per the pump-on cycle. The lock-in amplifier obviously

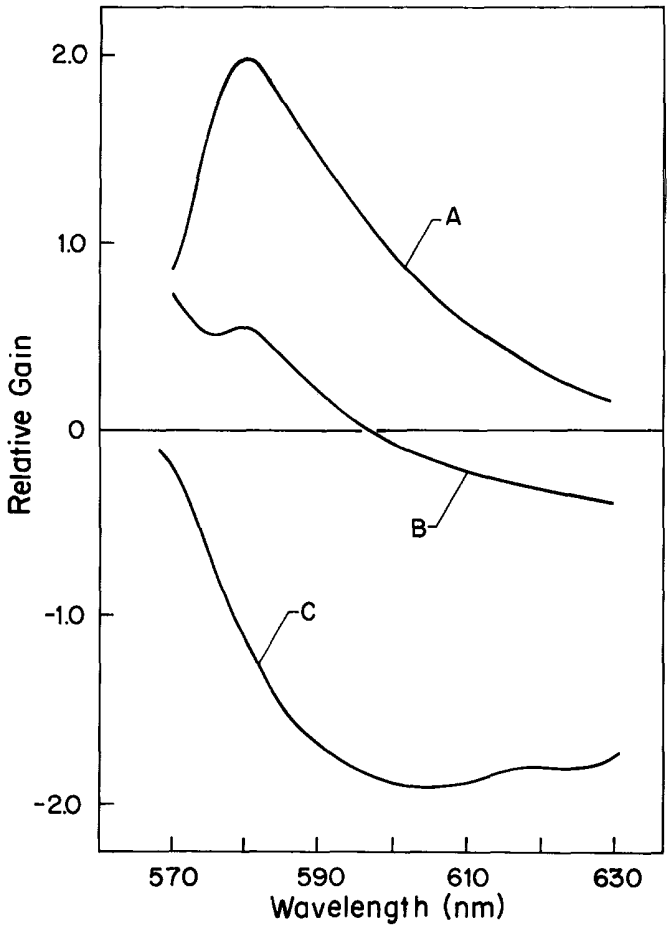

FIG. 8. Effect of triplet-triplet absorption losses on the pump/probe spectrum of rhodamine 6G: A, no KI added; B, 1×10^{-2} M KI added; C, 3×10^{-2} M KI added.

cannot follow the picosecond pulses but instead monitors the modulation in the amplitude envelope. Since the free temporal range is 13 ns and the delay line is 14 ns long, relative phases from 0° to 360° can be produced.

Example decay data for acridine red, $\tau = 3.3$ ns, and cresyl violet, $\tau = 2.6$ ns, are shown in Fig. 6. There are two complications in obtaining decay data. First, a zero phase lag between the two beams corresponds to a time delay of ~10 ns. This means that the decay is actually recorded starting at 20–25% of the way into the free temporal range. As a result, the data shown in Fig. 6 have been rearranged into a more natural sequence. The dashed line represents the extreme positions of the delay line. Second, the lack of continuity is the result of the delay-dependent probe focal size described in the experimental section. Ordinarily this artifact is removed from the data. It remains in Fig. 6 to indicate the magnitude of the needed correction. Time resolution is limited on the short end by the 250-ps argon-ion pump pulse, while the long end is restricted by the 13-ns free temporal range. Ostensibly the 250-ps width should allow the reliable determination of decays as short as 10 ps with the use of convolute and compare techniques. Unfortunately, this is difficult to demonstrate since most subnanosecond emitters have high intersystem crossing yields. The resulting large triplet concentration gener-

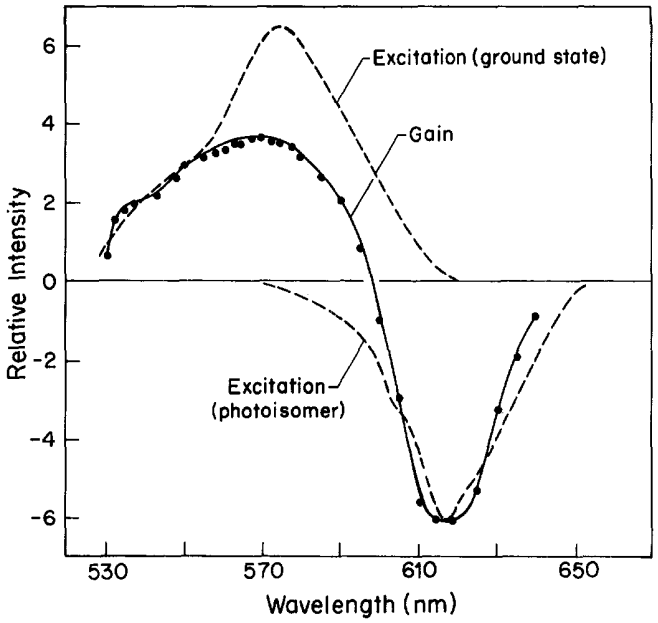

FIG. 9. Pump/probe spectrum of DODCI and its photoproduct. Note that zero intensity refers to the amplitude of the induced modulation and does not imply a transparent solution.

ates a signal which swamps out those due to excited-singlet processes. However, other fast phenomena such as rotational diffusion can be and have been observed. That is why it is necessary to adjust the relative polarization to the magic angle.[9] The free temporal range causes one decay to extend beyond the next pump pulse. Although for an exponential functionality the lifetime can still be extracted, the depth of modulation will be reduced. As an example of such difficulty, it has not yet been possible to record a spectrum for tris(2,2′-bipyridine)-Ru(II)Cl_2, which has an ~150 ns lifetime in air-saturated water.

Excited-State/Excited-State Transitions. Consider a three-state experiment where the pump pulse is absorbed by the sample and promotes an $S_0(v = 0) \rightarrow S_1^*$ $(v = n)$ transition. If the probe wavelength only corresponds to an excited-singlet-state absorption, e.g., S_1^* $(v = 0) \rightarrow S_2^*(v = m)$, it will be attenuated during the pump-on cycle (see Fig. 2C). The relationship between the probe amplification, singlet-state molar absorptivity, ϵ_s, and energy level concentrations can be written as

$$(T - 1)\alpha\epsilon_s[C_2^m(\text{on}) - C_1^0(\text{on})] - \epsilon_s[C_2^m(\text{off}) - C_1^0(\text{off})]. \quad (12)$$

Since $C_1^0(\text{off})$, $C_2^m(\text{off})$, and $C_2^m(\text{on})$ can all be approximated as zero, Eq. 12 reduces to the simple expression

$$(T - 1)\alpha - \epsilon_s C_1^0(\text{on}). \quad (13)$$

It can be seen that ϵ_s represents an attenuation as expected (see Fig. 3E). Thus, the net amplification for all singlet processes can be described by

$$(T - 1)\alpha(\epsilon_g - \epsilon_s)C_1^0(\text{on}). \quad (14)$$

This is shown in Fig. 3F.

The pump/probe spectra of rhodamines B and 6G possess inverted features due to $S_1^*(v = 0) \rightarrow S_4^*$

($v = 0$) transitions. Figure 7A shows this peak as occurring at 575 nm in rhodamine B. The $S_1^*(v = 0)$ state energy of the molecule combined with the probe photon energy, predicts that $S_4^*(v = 0)$ is 35,000 cm^{-1} in energy above the ground state. This result agrees with the value of 35,700 ± 400 cm^{-1} reported by Lin and Topp, using spontaneous fluorescence measurements.[14] Figure 7B shows that rhodamine 6G has an analogous and better-defined band at 570 nm. Again, this corresponds to a 36,000 cm^{-1} energy level and agrees quite well with the 36,200 ± 400 cm^{-1} value previously reported for the S_4^* state.[14]

A three-state absorption experiment can be envisioned where the probe wavelength now corresponds to a $T_1(v = 0) \rightarrow T_2(v = k)$ excited-triplet-state absorption (see Fig. 2C). The amplification can then be written as

$$(T - 1)\alpha - \epsilon_t C_t^0(\text{on}) \qquad (15)$$

where ϵ_t is the triplet-state molar absorptivity, and $C_t^0(\text{on})$ is the concentration of the lowest triplet state. Again, the concentration of $T_2(v = k)$ is considered to be negligible throughout the pump cycle, and $C_t^0(\text{off})$ is cautiously assumed to be zero. The overall behavior of a compound signal can then be described by

$$(T - 1)\alpha(\epsilon_g - \epsilon_s)C_1^0(\text{on}) + (\epsilon_a - \epsilon_t)C_t^0(\text{on}) \qquad (16)$$

as long as $S \leftrightarrow T$ interactions are negligible. For nanosecond singlet lifetimes and microsecond triplet lifetimes, the temporal behavior of $C_1^0(\text{on})$ and $C_t^0(\text{on})$ as a function of probe delay will be different. The singlet signal will usually decay as a function of delay because the corresponding lifetime is less than the free temporal range of the instrument. The triplet signal will usually remain constant since ~100 pump pulses will be required to reach a steady-state condition. Thus, $C_t^0(\text{on})$ represents the average value over the entire pump-on cycle.

The pump/probe spectra shown in Fig. 8 are for rhodamine 6G quenched by potassium iodide. Curve A is for no quencher added and corresponds to the situation where $C_t^0(\text{on}) \simeq 0$. Curve B has 10^{-3} M quencher added and demonstrates an intermediate case of Eq. 16, where all processes are contributing to the signal. Note that at 596 nm there are equal magnitude gains and losses. We term such wavelengths isometric points. For curve B this spectral feature will depend upon the relative phasing of the pump and probe pulses due to the $C_1^0(\text{on})$ term contribution, and will be concentration-dependent, since $C_t^0(\text{on})$ is produced via a second-order reaction. Finally, curve C is for 3×10^{-2} M quencher and demonstrates the case where the singlet contribution to the signal is small compared with that of the triplet. The resultant data agree with the published triplet-triplet absorption spectrum.[15,16] It should be noted that curve B can be made to resemble curve C by the use of a large relative phase angle to reduce the contribution of the $(\epsilon_g - \epsilon_s) \cdot C_1^0(\text{on})$ term.

Photoproduct Transitions. When the pump absorption results in photochemistry, both the reactants and products can contribute to the spectrum. Figure 9 shows the data for DODCI, including the parent excitation and photoisomer excitation spectra.[17] For this case, it appears that ground-state absorption accounts for most of the observed spectrum, with the isometric point occurring where the two molar absorptivity-concentration terms cancel. With this system the relative phasing between the pump and probe pulse trains has no effect on the signal. This is not surprising since the steady-state photoproduct concentration will be much larger than any transient excited-state concentration. In this specific case, the recovery of the ground state of the parent molecule during the pump-off cycle is not due entirely to a dark back reaction of the photoproduct but includes the replenishing of the sample by the rotation of the cell. It is interesting to note that with the use of this dye, the isometric point at 598 nm is within the wavelength region passively mode-locked. Examination of several other mode-locking dyes substantiates this observation, although it is not clear why there should be a correlation.

Instrumental Improvements. To improve the scope of the measurements obtained with the present configuration of the instrument, one could make several changes. The simplest would be the use of an achromatic lens pair to collimate the two beams through the sample cell. This would allow the use of effective molar absorptivities in quantitative studies. A slightly more involved modification would be the addition of a second dye laser to act as the pump. This would permit the separation of stimulated emission from absorption, since the probe could be fixed at a fluorescence wavelength and a spectrum recorded while the pump was scanned. The major trade is the increased cross-section for nonlinear processes because of improved temporal pulse overlap. Thus, two-photon absorption and Raman absorption would appear along with all of the other spectral transition types demonstrated earlier. Separating the total signal into each of its component parts could be a major task, requiring a sophisticated computer model. A final modification to improve the scope of the measurements would be the addition of cavity-dumping to the dye lasers. To obtain spectra having a reduced triplet contribution, one could increase the free temporal range to a few microseconds while still using the delay line to monitor singlet processes. To obtain triplet spectra free of fluorescence, one would control the timing between the pump and probe by the dumper electronics and not the delay line. This would permit the obtaining of triplet decays and/or spectra at 13 ns intervals. The free temporal range would be kept at a few microseconds.

To improve the signal-to-noise ratio of the measurements, one could make one simple change in the instrument. A higher modulation frequency, entailing a more expensive lock-in amplifier, would reduce laser noise, spinning cell noise, and the interference due to the ac thermal lens. In fact, chopping both of the beams and measuring the induced beat frequency should produce near-optimum results.[18,19] This latter scheme would require the expense of another modulator and additional signal-processing circuitry.

ACKNOWLEDGMENT

This work was supported in part by the National Science Foundation Grant CHE-8024635. The authors are indebted to R. B. Gregory for his help with the electronic design.

1. J. D. Wright, J. Chem. Ed. **11**, 894 (1982).
2. F. E. Lytle, J. Chem. Ed. **11**, 915 (1982).
3. T. Imasaka and N. Ishibashi, Reviews in Analytical Chemistry, Vol. VI, No. 4, 298 (1982).
4. A. Owyoung, IEEE J. Quantum Electronics **14**, 192 (1978).
5. D. Ricard, W. D. Lowdermilk, and J. Ducuing, Chem. Phys. Lett. **17**, 616 (1971).
6. H. E. Lessing, A. von Jena, and M. Reichert, Chem. Phys. Lett. **36**, 517 (1975).
7. C. V. Shank, E. P. Ippen, and O. Teschke, Chem. Phys. Lett. **45**, 291 (1977).
8. W. T. Barnes and F. E. Lytle, Appl. Phys. Lett. **34**, 509 (1979).
9. H. E. Lessing and A. von Jena, in *Laser Handbook*, M. L. Stitch, Ed. (North-Holland Publishers, New York, 1979), Vol. 3, Chap. B6.
10. G. R. Fleming, Adv. Chem. Phys. **49**, 1 (1982).
11. B. F. Levine, C. V. Shank, and J. P. Heritage, IEEE J. Quantum Electronics, **15**, 1418 (1979).
12. J. N. Eckstein, A. I. Ferguson, and T. W. Hansch, Phys. Rev. Lett. **40**, 847 (1978).
13. M. Hassinger and F. E. Lytle, Opt. Commun. **48**, 125 (1983).
14. H.-B. Lin and M. R. Topp, Chem. Phys. Lett. **47**, 442 (1977).
15. A. K. Chibisov and T. D. Stavnova, J. Photochem. **8**, 285 (1978).
16. D. N. Dempster, T. Morrow, M. F. Quinn, J. Photochem. **2**, 343 (1973/74).
17. D. N. Dempster, T. Morrow, R. Rankin, and G. F. Thompson, J. Chem. Soc. Faraday II **68**, 1479 (1972).
18. P. Bado, S. B. Wilson, and K. R. Wilson, Rev. Sci. Instrum. **53**, 706 (1982).
19. L. Andor, A. Lorinca, J. Siemion, D. D. Smith, and S. A. Rice, Rev. Sci. Instrum. **55**, 64 (1984).

Two-Frequency CARS for Mixture Analysis Using Pentacene in *p*-Terphenyl as a Model*

JACK K. STEEHLER and JOHN C. WRIGHT†
Department of Chemistry, University of Wisconsin, Madison, Wisconsin 53706

The usefulness of multiresonant nonlinear spectroscopy for analyzing complicated mixtures requires understanding of the factors controlling the relative signal positions and intensities of individual components. In this study the effects of different types of detuning from resonance, of the interactions of such detunings, and of the incident laser powers are illustrated. CARS spectra specific to the different pentacene sites in *p*-terphenyl are observed for different types of detunings from resonance, and the complications introduced by multiple components are interpreted. Population changes at moderate laser powers due to resonance with the allowed S_0 to S_1 transition lead to striking changes in the observed spectra, and markedly affect the interpretation of the observed resonances.

Index Headings: **Dye lasers; Nonlinear spectroscopy; Raman spectroscopy.**

INTRODUCTION

The experimental work of Hochstrasser *et al.*[1-3] and the theoretical work of Taran and others[4-8] demonstrate that multiresonant nonlinear spectroscopy has the capability of providing site-selective spectroscopy in complex mixtures. Such a capability would be analogous to the site-selective fluorescence techniques[9-12] that have been developed for a variety of fluorescent materials, but would have the distinct advantage of being applicable to nonfluorescent molecules or to systems with strong quenching. As is the case with fluorescence line narrowing, site selectivity in nonlinear spectroscopy would give line narrowing in the broad-line systems typical of practical sampling matrices. Site-selective nonlinear spectra would be obtained by the selection of one laser frequency to be resonant with the desired site or component in a mixture while a second laser frequency was scanned to provide the nonlinear spectrum of the selected site. Contributions from other sites or components would be discriminated against by the size of a single resonance enhancement. More generally, the use of three independent laser frequencies would provide the maximum selectivity in a four-wave mixing experiment because two resonance enhancements can be used to discriminate between the sites or components.

The extension of nonlinear techniques to site-selective spectroscopy is considerably more complicated than the extension of the fluorescence techniques. A number of different factors must be considered. For any selection of laser frequencies, there are several different types of multiple resonance that can occur in a CARS experiment involving different combinations of molecular energy levels (Fig. 1).[4-6,13] Each different type of resonance can lead to enhancement of the contribution from a particular site or component for an appropriate choice of laser frequencies. Understanding and predicting the positions and intensities of multiple resonances is crucial for studying multicomponent systems, since a single component can become multiply enhanced at several different frequency values. This understanding strongly affects the best choice of laser frequency for selectivity and for freedom from power-induced distortions of spectra.

Additionally, the level population changes that accompany multiresonant nonlinear methods make additional excited-state nonlinear processes possible. These induced population changes have been totally avoided in most published work to date, allowing a clearly defined initial state.[2,3,14] Excited-state CARS with resonant

Received 20 June 1984.
* This work was supported by the National Science Foundation under grants CHE81-19893 and CHE83-06084.
† Author to whom correspondence should be sent.

0003-7028/85/3903-0451$2.00/0